

# Submillimeter-Wave Sideband Generation Using Varactor Schottky Diodes

David S. Kurtz, *Member, IEEE*, Jeffrey L. Hesler, *Member, IEEE*, Thomas W. Crowe, *Senior Member, IEEE*, and Robert M. Weikle, II, *Member, IEEE*

**Abstract**—A submillimeter-wave sideband generator based on phase modulation is described. The sideband generator consists of a whisker-contacted Schottky varactor mounted in a reduced-height waveguide. A microwave pump signal modulates the reflection coefficient the varactor presents to an incident submillimeter-wave carrier. The circuit discussed in this paper has exhibited a carrier-to-single sideband conversion loss of 14 dB and an output power of 55  $\mu$ W at 1.6 THz.

**Index Terms**—Parametric upconverters, sideband generation, submillimeter-wave sources, varactor diodes.

## I. INTRODUCTION

INSTRUMENTATION needs in the radio-astronomy and remote-sensing communities have steadily increased the demand for local-oscillator sources operating at millimeter and submillimeter wavelengths [1], [2]. In addition, applications such as molecular spectroscopy [3], [4], detection and monitoring of chemical and biological warfare agents [5], and scaled radar-range techniques [6] have placed new emphasis on sources capable of broad frequency coverage. Unfortunately, tunable sources of submillimeter-wave radiation are uncommon. Far-infrared lasers operate at discrete spectral lines with typically no more than 200 MHz of tunable bandwidth [7]. Tunable solid-state sources and frequency multipliers usually exhibit poor efficiencies and produce relatively small output powers as their operating frequencies approach 1 THz [8], [9]. Sideband generation provides an alternative and attractive method for obtaining broadly tunable terahertz signals by mixing a fixed-frequency submillimeter-wave source with a tunable low-frequency (microwave) oscillator.

Sideband generators based on Schottky diode resistive mixers have been used for a number of years and have produced useful and tunable radiation at terahertz frequencies, but with relatively high conversion loss and limited output power. As an example, a whisker-contacted 1T15 Schottky diode fabricated at the University of Virginia (UVA), Charlottesville, and mounted in a corner-cube antenna has given 10.5- $\mu$ W of sideband power with a carrier-to-sideband conversion loss of 30 dB [10]. The power

output, in principle, can be improved by using a power-combining array of sideband generators, but this necessitates the use of a high-power pump source [11]. A different approach that has outstanding potential for improving sideband generator performance is based on parametric frequency conversion using a pumped nonlinear reactance.

Frequency upconverters based on varactor parametric devices have been a subject of interest since the early 1960s. The fundamental theory of the abrupt-junction varactor upconverter was described by Penfield and Rafuse in 1962 [12]. Initially, the interest in parametric upconverters focused on their application to multichannel frequency-division communication systems. Consequently, researchers gave considerable attention to the intermodulation properties and dynamic range of these devices in the microwave region [13]–[15]. Others have studied the conditions for optimum conversion efficiency, including the effects of embedding impedances and pump-power level [16]–[18]. Advances in diode-based resistive mixers and the development of microwave and millimeter-wave field-effect transistors during the 1970s and 1980s largely eliminated the need for and use of parametric upconverters for communications. Varactor-based sideband generation, however, remains a viable and attractive technique at submillimeter wavelengths, which lie significantly beyond the operating range of modern transistors.

In this paper, we present a submillimeter-wave sideband generator that utilizes the pumped nonlinear reactance of a Schottky varactor diode. The proof-of-principle circuit described in this paper has shown a single-sideband conversion loss of 14 dB with an output power of 55  $\mu$ W at 1.6 THz. These results represent an improvement of nearly 17 dB in conversion loss and a factor of five in power output over the best previously reported results that were based on resistive mixing [10].

## II. BACKGROUND AND SIMULATIONS

Fundamentally, a sideband generator is a modulator designed to convert power from a fixed carrier frequency to an upper or lower sideband. This frequency conversion may be accomplished by modulating either the amplitude or phase (or both) of a carrier wave with an applied pump signal. Consequently, the circuit and device design parameters affecting the performance of sideband generators are similar to those for resistive mixers and frequency multipliers. In particular, the conversion loss of a sideband generator depends on the impedance terminations at each sideband frequency, as well as the waveform of the pump signal.

Barber [19] and Saleh [20] have shown that minimum conversion loss for a resistive mixer with all sidebands terminated

Manuscript received September 24, 2002; revised February 27, 2002. This work was supported by the Army Research Office under Grant DAAG55-98-1-0489, by the National Science Foundation under Grant ECS 9623893 and Grant AST 9987104, and by the U.S. Army National Ground Intelligence Center under Grant DAHC90-96-C-0010.

D. S. Kurtz is with Virginia Diodes Inc., Charlottesville, VA 22903 USA.

J. L. Hesler, T. W. Crowe, and R. M. Weikle, II are with the School of Engineering and Applied Science, University of Virginia, Charlottesville, VA 22904 USA.

Digital Object Identifier 10.1109/TMTT.2002.804511

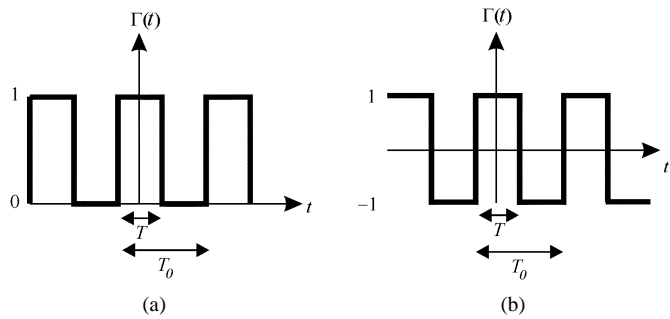


Fig. 1. Reflection coefficient representing: (a) a binary amplitude-shift-keying modulator and (b) a binary phase-shift-keying modulator. The power in the first sideband is maximized in both cases for a 50% duty cycle and yields a minimum conversion loss of 9.94 dB for (a) and 3.92 dB for (b).

in their optimum impedance occurs for a pump signal with low pulse-duty ratio. For typical sideband generators operating at submillimeter wavelengths, the pump signal is, for practical reasons, at a relatively low frequency (in the microwave or millimeter-wave range). This use of a low-frequency pump has important advantages and implications. In general, more power is available at microwave frequencies than at submillimeter-wave frequencies to modulate the impedance presented to the incident carrier. In addition, the parasitics associated with the varactor are usually not as significant at microwave frequencies as they are at submillimeter wavelengths. Most significantly, a low-frequency pump signal applied to the sideband generator results in an output spectrum consisting of a large number of closely spaced sidebands around the submillimeter-wave carrier. As a consequence, it is difficult or impractical to control the embedding impedance presented to each relevant sideband. A pragmatic approach is to terminate all sideband frequencies with identical matched loads. This results in a simple and broad-band circuit with reasonable embedding impedances. Kelly has shown that a lossless mixer with all sidebands terminated in matched loads and conductance driven between a perfect open-circuit and a perfect short-circuit performs best at a 50% duty cycle and yields a minimum conversion loss of 3.92 dB [21].

The lossless mixer described by Kelly gives a practical limit on submillimeter-wave sideband generator performance and can be understood by examining the Fourier components of the modulation waveforms shown in Fig. 1. For varactor sideband generation, the microwave pump signal effectively modulates the reflection coefficient presented to an incident submillimeter-wave carrier. In Fig. 1(a), this reflection coefficient is switched between a perfect match and perfect open circuit. This situation corresponds to binary amplitude shift keying and is reminiscent of a carrier being modulated with an optical chopper. The conversion *gain* (in decibels) from the carrier to the upper or lower sideband is, in this case,

$$G_a = 20 \log \left| \frac{T}{T_0} \operatorname{sinc} \left( k \frac{T}{T_0} \right) \right| \text{ dB} \quad (1)$$

where  $k = 1$  for the first sideband,  $\operatorname{sinc}(x) = \sin(\pi x)/\pi x$ , and  $T/T_0$  is the pump duty ratio. Fig. 1(b) illustrates the case considered by Kelly in which a carrier is phase modulated by a pumped element whose reflection coefficient is switched be-

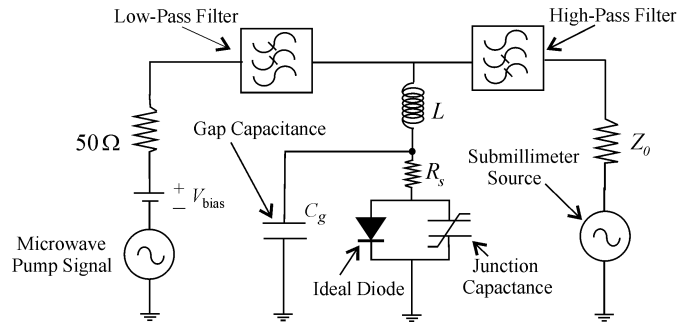


Fig. 2. Circuit model for a varactor sideband generator. The microwave pump and bias are applied through an ideal low-pass filter and the submillimeter carrier through an ideal high-pass filter. A series inductor resonates with the varactor to produce a phase variation of 180°.

tween a perfect open circuit ( $\Gamma = 1$ ) and a perfect short circuit ( $\Gamma = -1$ ). For this case,

$$G_b = 20 \log \left| 2 \frac{T}{T_0} \operatorname{sinc} \left( k \frac{T}{T_0} \right) \right| \text{ dB.} \quad (2)$$

For both types of modulation, the power converted to the first sideband is optimized with a 50% duty cycle, resulting in a minimum conversion loss of 9.94 dB for Fig. 1(a) and 3.92 dB for Fig. 1(b), as given by Kelly.

In most implementations, a sideband generator will be pumped with a sinusoidal microwave source rather than a square wave. Consequently, the conversion gain will be somewhat lower than the idealized situation described above. In addition, diode series resistance and reverse breakdown will degrade sideband generator performance to some extent. The simple circuit shown in Fig. 2 represents a basic implementation of a sideband generator and may be used to examine performance tradeoffs. The microwave pump source is assumed to have a 50-Ω impedance and the submillimeter-wave carrier (at 1.6 THz) is produced by a 120-Ω generator, corresponding to the TE<sub>10</sub>-mode impedance for the reduced-height waveguide that is used in this study. Typical GaAs whisker-contacted varactor diodes designed for operation at terahertz frequencies have zero-bias junction capacitance in the range of 5–15 fF, series resistance on the order of 10 Ω, and breakdown voltages of 8–15 V. The inductance in the circuit represents a whisker contact and is chosen to resonate with the varactor, producing a large phase variation (ideally, 180°). Since the series resistance is a function of the depletion region width, designing the inductor to resonate with the varactor when the active region is fully depleted minimizes power dissipation in the diode.

The circuit shown in Fig. 2 was simulated using Applied Wave Research's Microwave Office (version 4.0).<sup>1</sup> The varactor was treated as an ideal nonlinear capacitor with a junction potential of 1 V and grading parameter of 0.5 (corresponding to an abrupt junction). The nonlinear conductance of the Schottky junction was modeled as the standard exponential dependence with an ideality factor of 1.2 and reverse breakdown voltage of 10 V. Fig. 3(a) shows the predicted conversion gain of the sideband generator as a function of pump power for different values of junction series resistance. The diode series resistance and

<sup>1</sup>Applied Wave Research Inc., El Segundo, CA. [Online] Available: <http://www.appwave.com>

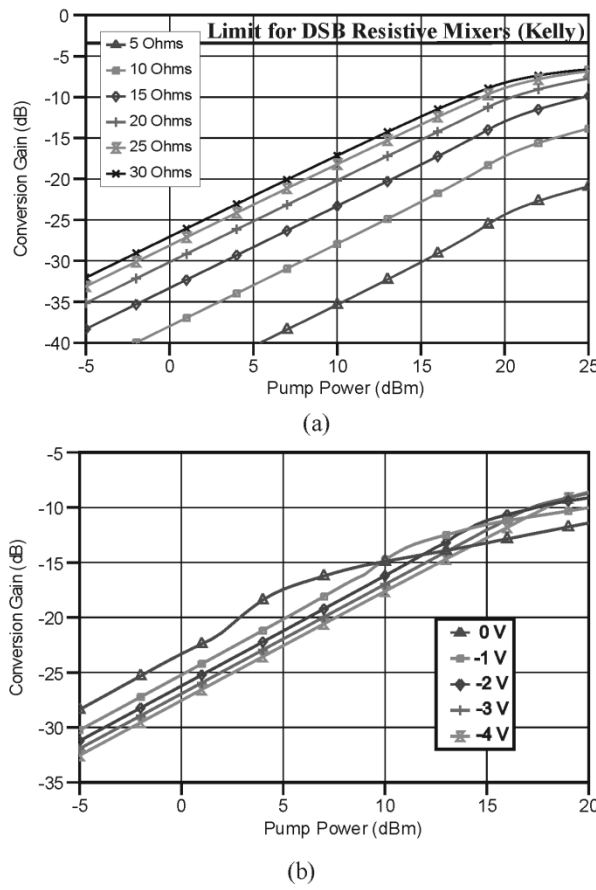


Fig. 3. (a) Conversion gain versus available pump power of a varactor sideband generator for different values of series resistance. The reverse-bias voltage is  $-5$  V and the zero-bias junction capacitance is directly related to  $R_s$  by the cutoff frequency. (b) Conversion loss versus available pump power for different bias voltages and a series resistance of  $25$   $\Omega$ . For these simulations, the submillimeter source impedance  $Z_0$  is set to  $120$   $\Omega$  (corresponding to the  $TE_{10}$ -mode impedance in the reduced-height waveguide), the series inductance is  $15$   $pH$  (reactance of  $150$   $\Omega$  at  $1.6$  THz), and the parasitic gap capacitance  $C_g$  is neglected. The submillimeter-wave source frequency is  $1.6$  THz and the microwave pump signal is fixed at  $2$  GHz.

junction capacitance are not independent and the results shown in Fig. 3 assume the diode has a fixed cutoff frequency  $f_c$  of  $3.5$  THz, where  $f_c$  is given by the usual expression

$$f_c = \frac{1}{2\pi R_s C_{j0}} \quad (3)$$

with  $R_s$  being the diode series resistance and  $C_{j0}$  being the zero-bias junction capacitance. For comparison, the conversion loss limit derived by Kelly is also shown.

Fig. 3(b) shows the simulated sideband generator conversion gain versus available pump power for different bias voltages. Clearly, sideband generator conversion gain improves with increasing pump power (at  $10$  dB per decade for low pump levels), saturating as the pump voltage amplitude approaches the bias voltage. At high pumping levels, the varactor impedance is modulated over a larger range of values, producing a greater phase variation in the reflection coefficient presented to the submillimeter carrier. Fig. 4 illustrates the sideband conversion loss as a function of microwave pump power for different values of the

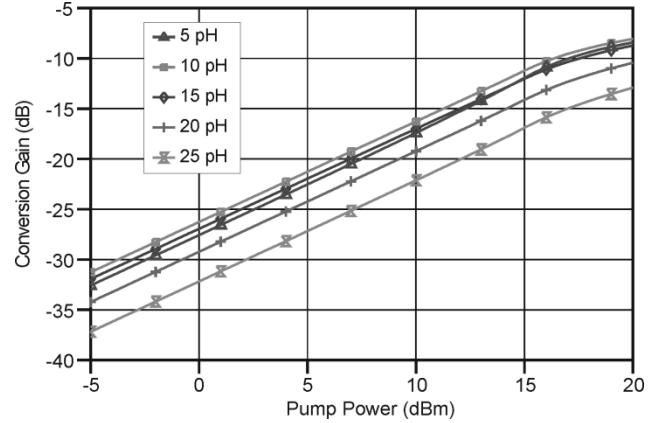


Fig. 4. Simulated conversion gain versus available pump power for the varactor sideband generator as a function of series inductance  $L$ . In this simulation, the submillimeter and microwave pump frequencies are  $1.6$  THz and  $2$  GHz, respectively, the series resistance is fixed at  $25$   $\Omega$  (which corresponds to  $C_{j0}$  of  $1.8$  fF), the bias voltage is  $-3$  V, and the parasitic gap capacitance  $C_g$  is neglected.

post series inductance  $L$ . For the simulations shown in Figs. 3 and 4, the microwave pump frequency is  $2$  GHz and the submillimeter-wave source is fixed at  $1.6$  THz.

For low-sideband generator conversion loss, it is important that the junction capacitance of the varactor resonate with the post inductance at the submillimeter carrier frequency. It is worth noting and is evident in Fig. 3(a) that, given a series inductance, a relatively large series resistance can be tolerated to achieve the necessary junction capacitance so long as this resistance is significantly smaller than the impedance of the submillimeter-wave source. Reducing the height of the waveguide further (and, thus, reducing  $Z_0$ ) would permit the use of varactor diodes with larger anode diameters (and correspondingly larger  $C_{j0}$  and smaller  $R_s$ ). However, in this study, the practical decision to limit waveguide dimensions to half-height was made to facilitate fabrication and assembly of the circuit.

### III. DESIGN CONSIDERATIONS

The varactor sideband generator presented in this paper is based upon the circuit shown in Fig. 2 and was implemented in a reduced-height waveguide using a whisker-contacted varactor diode. A diagram of the basic structure is shown in Fig. 5(a). An initial design was implemented using the waveguide mount model developed by Eisenhart and Khan [22] and this was refined using Ansoft Corporation Inc.'s High Frequency Structure Simulator (HFSS).<sup>2</sup> The use of a planar Schottky varactor would allow easier assembly of the circuit, but the presence of the high-permittivity GaAs substrate introduces a large parasitic capacitance across the diode junction that, in simulations, dramatically degrades the performance of the sideband generator. Consequently, the circuit described in this paper employs a planar whisker contact similar to that developed at the Rutherford Appleton Laboratory, Oxfordshire, U.K., by Mann *et al.* [23].

<sup>2</sup>Ansoft Corporation Inc., Pittsburgh, PA. [Online] Available: <http://www.ansoft.com>

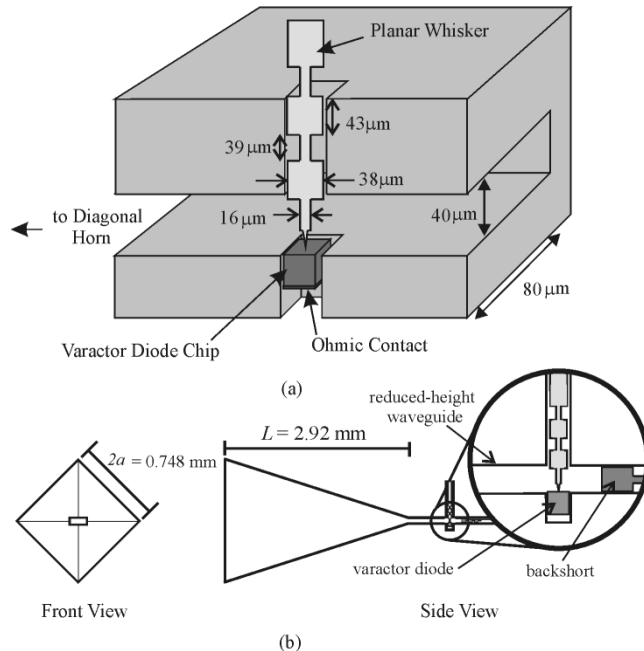


Fig. 5. (a) Diagram showing one-half of the sideband generator waveguide housing. A varactor diode chip is mounted to the waveguide housing with conductive epoxy and a planar whisker extends across the waveguide channel to make contact. (b) Diagram of the integrated diagonal horn showing the horn length  $L$  and aperture parameter  $a$ .

#### A. Waveguide Design

To produce a full  $180^\circ$  phase shift, the series combination of the varactor and whisker inductance shown in Fig. 2 must be tuned from a high impedance to a low impedance relative to  $Z_0$ , i.e., the characteristic impedance of the submillimeter waveguide. Given typical and realistic submillimeter varactor equivalent-circuit parameters, it is difficult to achieve large impedances relative to the full-height TE<sub>10</sub>-mode impedance of  $240 \Omega$ . Consequently, a half-height waveguide (dimensions of  $40 \times 160 \mu\text{m}$ ) was chosen as the propagation medium for the sideband generator. With these dimensions, the waveguide exhibits single-mode propagation over the 1190–1746-GHz band.

The waveguide block was fabricated through electroforming by Custom Microwave Inc.<sup>3</sup> and included an integrated diagonal feedhorn to couple the submillimeter-wave carrier from a far-infrared laser to the varactor [see Fig. 5(b)]. The feedhorn, which has a length  $L$  of 2.92 mm and aperture dimension  $a$  of 0.374 mm, was designed based on the work by Johansson and Whyborn [24]. HFSS simulations were performed to verify that the reduced-height waveguide is not cut off where the horn introduces a section of a notched waveguide in the transition region between the antenna and rectangular guide. The waveguide channel between the planar whisker and feedhorn (200 μm in length) was chosen to be short enough to minimize sidewall losses, but sufficiently long to allow decay of the evanescent fields in the vicinity of the varactor.

To permit adjustment of the impedance presented to the varactor, the waveguide design included a tunable backshort. The backshort was fabricated by plating copper through a

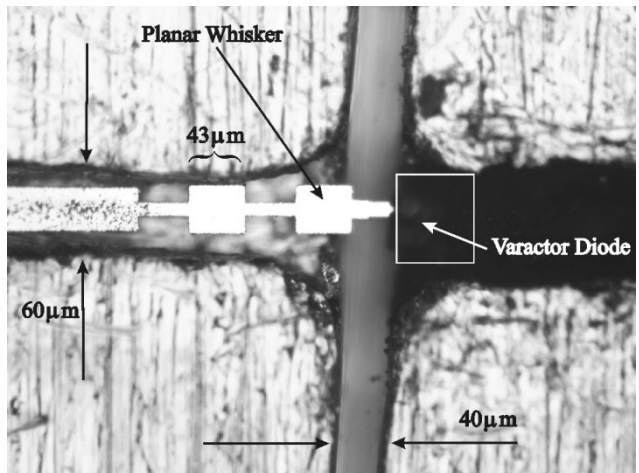


Fig. 6. Photograph of the sideband generator. The microwave pump signal is feed through a low-pass filter to a planar whisker that contacts a varactor diode chip.

photolithographically defined mask onto a silicon substrate with sputtered chrome/gold seed layer. The plating mask was formed from an ultra-thick negative photoresist SU-8 [25]. After plating, the backshort was removed from the SU-8 mold and soldered to a brass post connected to a micrometer.

#### B. Planar Whisker Design and Fabrication

Electrical contact to the varactor is provided through a planar whisker, shown in Figs. 5 and 6. A low-pass filter is integrated into the whisker to prevent the submillimeter carrier from propagating to the microwave pump source. This filter was designed with the aid of HFSS and the relevant dimensions are shown in Fig. 5. The width of the whisker (16 μm) was chosen to provide the inductance needed to resonate with the varactor without introducing a significant gap capacitance  $C_g$  that would shunt the diode. To allow sufficient force for contacting the varactor anodes without being too large to fit into the anode well, the whisker tapers to a point and has a thickness between 85%–90% of the anode diameter [23]. The length of the taper was chosen to minimize the parasitic gap capacitance ( $C_g$ ) across the diode without exceeding 25% of the waveguide height, which is the criterion given by Eisenhart and Khan for validity of their waveguide mount model [22].

The planar whiskers were fabricated by sputtering approximately 700 nm of chrome and gold onto a quartz substrate. The whiskers were then patterned photolithographically with an AZ P4110 photoresist and defined by a wet chemical etch. The portion of the whiskers containing the low-pass filter and waveguide probe (but excluding the taper) was gold plated to a thickness of several micrometers (approximately 2.5 μm) to reduce ohmic losses and provide greater tensile strength for contacting the varactor anodes. Finally, the quartz substrate was dissolved in hydrofluoric acid (49% solution) to release the whiskers.

#### C. Varactor Design and Mounting

Since the phase modulation produced by the sideband generator results from resonance between a varactor and the series inductance of the whisker, the junction capacitance of the diode

<sup>3</sup>Custom Microwave Inc., Longmont, CO. [Online] Available: <http://www.custommicrowave.com>

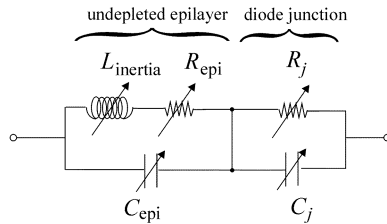


Fig. 7. High-frequency circuit model for a varactor diode [26].  $R_{\text{епи}}$  and  $C_{\text{епи}}$  represent the conduction and displacement currents through the undepleted epitaxial region.  $L_{\text{inertia}}$  models the carrier inertia. All components are functions of the junction voltage. In the above expressions,  $t_e$  is the epilayer thickness,  $x_d$  is the depletion width,  $A$  is the diode area,  $\epsilon$  is the permittivity,  $m^*$  is effective mass,  $q$  is the fundamental unit of charge,  $\mu$  is mobility, and  $\sigma_e$  is the conductivity of the epitaxial layer.

is the critical design parameter. At submillimeter wavelengths, it is also important to consider the parasitics associated with the diode mount, as well as effects such as carrier inertia and plasma resonance in the undepleted epitaxial region [26]. The equivalent circuit shown in Fig. 7 was used to model the varactor in this study. The component values are related to the device physical parameters, as shown in Fig. 7, and include a voltage-dependent resistor, inductor, and capacitor that represent both conduction and displacement current through the undepleted epilayer, as well as carrier inertia.

Carrier velocity saturation, which limits how fast a depletion region's width can be modulated, has a profound influence on submillimeter varactor multipliers operating at high-power levels [27], [28]. Velocity saturation, however, is not expected to play a significant role in the performance for varactor sideband generators due to the relatively low frequency of the modulating pump signal. Consequently, velocity saturation effects were neglected in the diode model used for this study.

The complete diode model of Fig. 7 was simulated using the Hewlett-Packard Company's Microwave Design System and the diode epilayer and anode contact were optimized for maximum sideband conversion efficiency. In these simulations, an equivalent circuit for the planar whisker, consisting of the series inductance  $L$  and gap capacitance  $C_g$ , shown in Fig. 2, was included. Resulting parameters of the varactor and whisker-embedding circuit for sideband generation at 1.6 THz are listed in Table I. Given these parameters, nominal values for the diode's epilayer circuit model elements at zero bias are  $R_{\text{епи}} = 18 \Omega$ ,  $C_{\text{епи}} = 0.4 \text{ fF}$ , and  $L_{\text{inertia}} = 2.7 \text{ pH}$ . The plasma frequency of the diode epilayer is calculated to be 4.7 THz. In addition, spreading resistance is expected to contribute approximately  $7 \Omega$  to the varactor's series impedance.

A GaAs varactor with the device parameters given in Table I was fabricated in the Semiconductor Device Laboratory, University of Virginia. An ohmic contact was fabricated on the backside and the wafer was diced into chips measuring  $50 \mu\text{m} \times 50 \mu\text{m} \times 75 \mu\text{m}$ . DC measurements indicated that the varactor had a series resistance of  $29 \Omega$  and a breakdown voltage of 7.8 V. The diode was mounted into the sideband generator waveguide block using conductive epoxy and cured at  $60^\circ\text{C}$  for 7 h. Contact was made to the anode by bonding the planar whisker onto a 1-mil-thick brass shim using conductive epoxy. The shim was attached to a probe and the whisker was

TABLE I  
OPTIMIZED DIODE AND PLANAR WHISKER PARAMETERS FOR SIDEband  
GENERATION AT 1.6 THz

|                                   |                                      |
|-----------------------------------|--------------------------------------|
| Anode diameter                    | $0.8 \mu\text{m}$                    |
| Doping                            | $2.3 \times 10^{17} \text{ cm}^{-3}$ |
| Epilayer thickness                | $0.21 \mu\text{m}$                   |
| Series resistance                 | $25 \Omega$                          |
| Junction Capacitance ( $C_{j0}$ ) | $1.0 \text{ fF}$                     |
| Post inductance                   | $16 \text{ pH}$                      |
| Gap Capacitance ( $C_g$ )         | $0.4 \text{ fF}$                     |

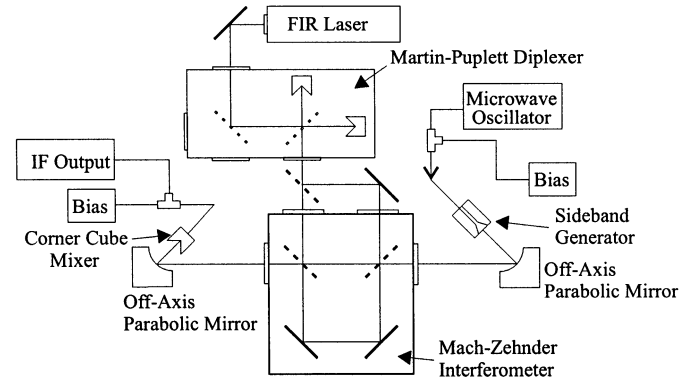


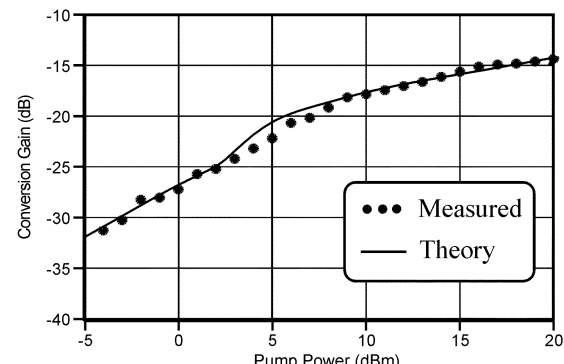
Fig. 8. Measurement setup for the 1.6-THz sideband generator. The Martin-Puplett diplexer is used to rotate the polarization of the laser output.

brought into contact with the varactor. This technique allows monitoring of electrical contact to the diode by connecting the probe to a curve tracer. Once contact is made, the shim is epoxied to a microstrip transmission line that lies further back along the waveguide cross channel.

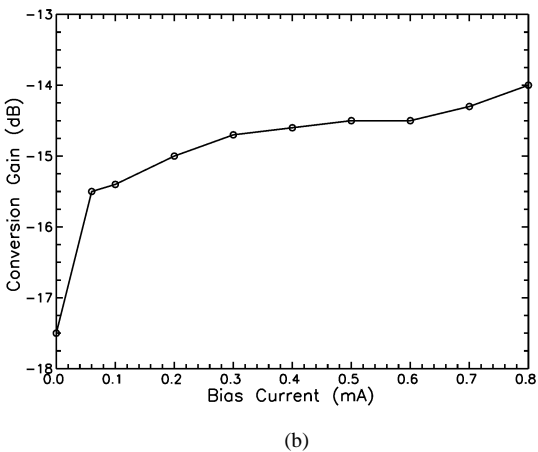
#### IV. MEASUREMENTS

The output power and conversion efficiency of the varactor sideband generator were measured using the experimental setup shown in Fig. 8. The submillimeter carrier was generated with a CO<sub>2</sub>-pumped far-infrared laser, which produced 3 mW of output power at 1.6 THz. This carrier passed through a 3-dB Mylar beam-splitter and the two resulting beams were directed into the input ports of a Mach-Zehnder interferometer. The arms of the interferometer were adjusted to provide half the laser power (1.5 mW) to the sideband generator. The remaining 1.5 mW of input laser power was used to drive a corner-cube mixer.

The submillimeter-wave carrier was focused into the diagonal feedhorn of the sideband generator block with an off-axis parabolic reflector and the microwave pump power was provided through a subminiature assembly (SMA) coaxial connection. The coupling efficiency to the diagonal horn was not accounted for in our measurements. Consequently, the submillimeter carrier power input to the sideband generator was taken to be the total power incident onto the face of the diagonal feed horn. The sidebands produced by the modulated varactor reradiate from the feedhorn and are focused back into the Mach-Zehnder interferometer, where they pass directly through to the corner-cube mixer.



(a)



(b)

Fig. 9. (a) Plot of the sideband generator conversion gain as a function of microwave pump power at 1.8 GHz. (b) Plot of the sideband generator conversion gain as a function of bias current. For this measurement the microwave pump power is 20 dBm and the pump frequency is 1.8 GHz.

The conversion loss (13-dB double sideband) and noise temperature of the corner-cube mixer were determined in a separate measurement using thermal radiation from a hot/cold blackbody source that filled the field-of-view of the corner-cube antenna. This measurement, which was repeated several times during the testing of the sideband generator, was found to be repeatable over a range of input local-oscillator powers to within a few tenths of a decibel. It should be noted that the gain of corner cubes can vary significantly from antenna-to-antenna due to variations in sidelobe radiation, which can be quite high. In addition, there will be a coupling loss between the input beam from the sideband generator and the receiving pattern of the corner cube. For the results presented below, the optics of the measurement system were adjusted to maximize the power received by the corner-cube mixer. However, no attempt was made to correct for coupling losses to the antenna or to account for other losses in the measurement system. Consequently, the measurements presented below should represent a conservative estimate for the power output and conversion efficiency of the sideband generator.

Fig. 9(a) shows the measured *single-sideband* conversion gain of the sideband generator as a function of microwave pump power. The sideband power incident on the corner cube was determined from the IF output using the measured conversion

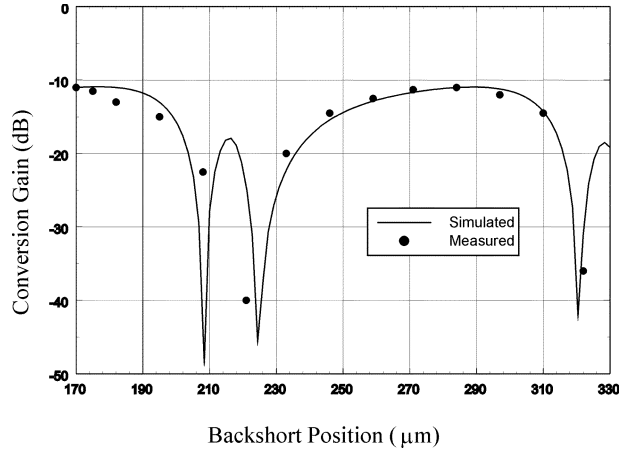


Fig. 10. Measured and simulated conversion gain versus backshort position. The conversion gain in this plot is double sideband.

loss of the mixer. With 20 dBm of microwave pump power, the varactor sideband generator produced an estimated 55  $\mu$ W of single-sideband output power with a carrier-to-sideband conversion gain of -14 dB. The theoretical curve was obtained using the software package Microwave Office with the diode and whisker parameters given in Table I. Fig. 9(b) shows the sideband generator performance as a function of dc-bias current. For this measurement, the diode was biased with a current source and then the microwave pump applied. Allowing the varactor to be driven slightly into forward conduction results in additional modulation of the junction capacitance and improves the sideband generator conversion efficiency [29]. For all these measurements, the microwave pump source was set to a fixed frequency of 1.8 GHz, corresponding to the IF amplifier and filter used for the corner-cube mixer.

The conversion gain of the sideband generator as a function of backshort position is shown in Fig. 10. Although, in typical applications, one sideband is usually filtered out, the corner-cube mixer combines both sidebands into the IF output. Phase differences between these mixing products that result from the propagation delay between the sideband generator and the mixer can have a significant effect on the measured IF output. The conversion gain shown in Fig. 10 is double sideband and, as is clear from the data, the backshort has a dramatic influence on the superposition of the upper and lower sideband mixing products.

## V. DISCUSSION

In this paper, we have described the application of varactor diodes to generating sideband radiation at submillimeter wavelengths. The technique uses a relatively simple resonant circuit to phase modulate an incident submillimeter-wave carrier. Although the fundamental idea is not new and has been investigated extensively at microwave frequencies, varactor sideband generation has not been exploited widely as a technique for producing tunable submillimeter radiation.

The varactor sideband generator studied in this paper has shown a carrier-to-single-sideband conversion loss of 14 dB and an output power of 55  $\mu$ W. It should be noted that the output power measured from the sideband generator was limited by the power available from the far-infrared laser. In principle, more

output power should be obtainable by simply replacing the laser with a higher power source. The results described above represent a 17-dB improvement in conversion loss and a fivefold improvement in output power over the previously reported best results at 1.6 THz, which were based on resistive mixing in a corner cube.

It is anticipated that future developments and application of planar diode processing technology as well as waveguide micro-machining techniques will lead to further improvements in the design, assembly, and performance of varactor sideband generators at submillimeter wavelengths.

#### ACKNOWLEDGMENT

The authors are grateful to W. Bishop, University of Virginia, Charlottesville, who fabricated the diodes used in this study and for the advice and help of D. Porterfield, Virginia Diodes Inc., Charlottesville, VA, K. Hui, Agere Systems Inc., Allentown, PA, and L. Suddarth, University of Virginia, Charlottesville.

#### REFERENCES

- [1] T. G. Phillips and J. Keene, "Submillimeter astronomy," *Proc. IEEE*, vol. 80, pp. 1662–1678, Nov. 1992.
- [2] J. W. Waters, "Submillimeter-wavelength heterodyne spectroscopy and remote sensing of the upper atmosphere," *Proc. IEEE*, vol. 80, pp. 1679–1701, Nov. 1992.
- [3] H. M. Pickett, "THz spectroscopy of the atmosphere," *Proc. SPIE-Int. Soc. Opt. Eng.*, vol. 3617, pp. 2–6, Jan. 1999.
- [4] J. T. Kindt and C. A. Schmuttenmaer, "Far-infrared dielectric properties of polar liquids probed by femtosecond THz pulse spectroscopy," *J. Phys. Chem.*, vol. 100, pp. 10 373–10 379, 1996.
- [5] N. Gopalsami and A. C. Raptis, "Millimeter-wave radar sensing of airborne chemicals," *IEEE Trans. Microwave Theory Tech.*, vol. 49, pp. 646–653, Apr. 2001.
- [6] M. J. Coulombe, T. Horgan, J. Waldman, G. Scatkowski, and W. Nixon, "A 520 GHz polarimetric compact range for scale model RCS measurements," in *Proc. Antenna Meas. and Tech. Assoc.*, Monterey, CA, Oct. 1999, pp. 118–123.
- [7] G. A. Blake, K. B. Laughlin, R. C. Cohen, K. L. Busarow, D. H. Gwo, C. A. Schmuttenmaer, D. W. Steyert, and R. J. Saykally, "The Berkeley tunable far infrared laser spectrometer," *Rev. Sci. Instrum.*, vol. 62, no. 7, pp. 1693–1700, July 1991.
- [8] T. W. Crowe, T. C. Grein, R. Zimmermann, and P. Zimmermann, "Progress toward solid-state local oscillators at 1 THz," *IEEE Microwave Guided Wave Lett.*, vol. 6, pp. 207–208, May 1996.
- [9] A. V. Räisänen, "Frequency multipliers for millimeter and submillimeter wavelengths," *Proc. IEEE*, vol. 80, pp. 1842–1852, Nov. 1992.
- [10] E. R. Mueller and J. Waldman, "Power and spatial mode measurements of sideband generated, spatially filtered, submillimeter radiation," *IEEE Trans. Microwave Theory Tech.*, vol. 42, pp. 1891–1895, Oct. 1994.
- [11] D. S. Kurtz, J. L. Hesler, J. B. Hacker, T. W. Crowe, D. B. Rutledge, and R. M. Weikle, II, "Submillimeter-wave sideband generation using a planar diode array," in *IEEE MTT-S Int. Microwave Symp. Dig.*, vol. 3, Baltimore, MD, 1998, pp. 1903–1906.
- [12] P. Penfield and R. P. Rafuse, *Varactor Applications*. Cambridge, MA: MIT Press, 1962.
- [13] B. S. Perlman, "Current-pumped abrupt-junction varactor power-frequency converters," *IEEE Trans. Microwave Theory Tech.*, vol. MTT-13, pp. 150–161, Mar. 1965.
- [14] S. M. Perlow and B. S. Perlman, "A large signal analysis leading to intermodulation distortion prediction in abrupt junction varactor upconverters," *IEEE Trans. Microwave Theory Tech.*, vol. MTT-13, pp. 820–827, Nov. 1965.
- [15] J. G. Gardiner and S. I. Ghobrial, "Distortion performance of the abrupt-junction current-pumped varactor frequency converter," *IEEE Trans. Microwave Theory Tech.*, vol. MTT-19, no. 9, pp. 741–749, Sept. 1971.
- [16] G. I. Matthaei, "A study of the optimum design of wide-band parametric amplifiers and up-converters," *IRE Trans. Microwave Theory Tech.*, vol. MTT-9, pp. 23–38, Jan. 1961.
- [17] A. Korpel and V. Ramaswamy, "Input conductance of a four-frequency parametric up-converter," *IEEE Trans. Microwave Theory Tech.*, vol. MTT-13, pp. 96–106, Jan. 1965.
- [18] A. I. Grayzel, "The overdriven varactor upper sideband upconverter," *IEEE Trans. Microwave Theory Tech.*, vol. MTT-15, pp. 561–565, Oct. 1967.
- [19] M. R. Barber, "Noise figure and conversion loss of the Schottky barrier mixer diode," *IEEE Trans. Microwave Theory Tech.*, vol. MTT-15, pp. 629–635, Nov. 1967.
- [20] A. A. M. Saleh, *Theory of Resistive Mixers*. Cambridge, MA: MIT Press, 1971.
- [21] A. J. Kelly, "Fundamental limits on conversion loss of double sideband resistive mixers," *IEEE Trans. Microwave Theory Tech.*, vol. MTT-25, pp. 867–869, Nov. 1977.
- [22] R. L. Eisenhart and P. J. Khan, "Theoretical and experimental analysis of a waveguide mounting structure," *IEEE Trans. Microwave Theory Tech.*, vol. MTT-19, pp. 706–719, Aug. 1971.
- [23] C. M. Mann, D. N. Matheson, B. N. Ellison, M. L. Oldfield, B. P. Moyna, J. J. Spencer, D. S. Wilsher, and B. J. Maddison, "On the design and measurement of a 2.5 THz waveguide mixer," in *Proc. 9th Int. Space Terahertz Tech. Symp.*, Pasadena, CA, Mar. 1998, pp. 161–171.
- [24] J. F. Johansson and N. D. Whyborn, "The diagonal horn as a sub-millimeter wave antenna," *IEEE Trans. Microwave Theory Tech.*, vol. 40, pp. 795–800, May 1992.
- [25] K. Y. Lee, N. LaBianca, S. A. Rishton, S. Zolgharnain, J. D. Gelorme, J. Shaw, and T. H.-P. Chang, "Micromachining applications of a high resolution ultrathick photoresist," *J. Vac. Sci. Technol. B, Microelectron. Process. Phenom.*, vol. B 13, no. 6, pp. 3012–3016, Nov./Dec. 1995.
- [26] T. W. Crowe, "GaAs Schottky barrier mixer diodes for the frequency range from 1–10 THz," *Int. J. Infrared Millim. Waves.*, vol. 10, no. 7, pp. 756–777, July 1989.
- [27] E. L. Kollberg, T. J. Tolmunen, M. A. Frerking, and J. R. East, "Current saturation in submillimeter wave varactors," *IEEE Trans. Microwave Theory Tech.*, vol. 40, pp. 831–838, May 1992.
- [28] J. T. Louhi and A. V. Räisänen, "On the modeling and optimization of Schottky varactor frequency multipliers at submillimeter wavelengths," *IEEE Trans. Microwave Theory Tech.*, vol. 43, pp. 922–926, Apr. 1995.
- [29] D. S. Kurtz, J. L. Hesler, T. W. Crowe, and R. M. Weikle, II, "Millimeter-wave sideband generation using varactor phase modulators," *IEEE Microwave Guided Wave Lett.*, vol. 10, pp. 245–247, June 2000.

**David S. Kurtz** (M'00) was born in Harrisonburg, VA, on October 12, 1970. He received the B.S. degree in electrical engineering, M.S. degree, and Ph.D. degree from the University of Virginia, Charlottesville, in 1992, 1997, and 2000, respectively. His graduate research focused on using quasi-optical techniques for multipliers and sideband generators to improve submillimeter-wave technology.

In October 2000, he joined Agilent Technologies Inc., Santa Rosa, CA, where he developed manufacturing test processes for new products including performance spectrum analyzers. He has been involved with determining and defining analyzer specifications for emerging communication standards. He is currently with Virginia Diodes Inc., Charlottesville, VA.



**Jeffrey L. Hesler** (S'88–M'89) was born in Seattle, WA, on July 8, 1966. He received the B.S.E.E. degree from the Virginia Polytechnic Institute and State University, Blacksburg, in 1989, and the M.S.E.E. and Ph.D. degrees from the University of Virginia, Charlottesville, in 1991 and 1996, respectively.

From 1989 to 1995, he was a Research Assistant with the University of Virginia, where he was involved with the development of waveguide and quasi-optical receivers. In 1997, he joined the School of Electrical Engineering and Applied Science, University of Virginia, as a Research Assistant Professor, where he is currently involved with research on submillimeter-wave receivers and multipliers.



**Thomas W. Crowe** (S'82–M'82–SM'95) received the B.S. degree in physics from Montclair State College, Montclair, NJ, in 1980, and the M.S.E.E. and Ph.D. degrees from the University of Virginia, Charlottesville, in 1982 and 1986, respectively.

In March 1986, he joined the faculty of the University of Virginia as a Research Assistant Professor of electrical engineering, and was promoted to Research Professor in August 1997. Since January 1989, he has been the Director of the Semiconductor Device Laboratory, and in 1996, he became Director of the Applied Electrophysics Laboratories. His career has focused on creating the technology necessary to open the terahertz portion of the electromagnetic spectrum for routine scientific and commercial exploitation. He has led the research team that has developed and fabricated many of the best GaAs Schottky barrier diodes for scientific applications including radio astronomy, plasma diagnostics, and studies of the chemistry of the upper atmosphere. His research team designed and created the diodes used on the highly successful submillimeter wave astronomy satellite (SWAS), as well as a number of Department of Defense (DoD) and European remote sensing satellites. The planar diode technology that is currently being developed is opening the way for greater levels of system integration and increased reliability, making possible a host of new applications in this critical frequency range. He is the founder and President of Virginia Diodes Inc., Charlottesville, VA.



**Robert M. Weikle, II** (S'90–M'91) was born in Tacoma, WA, in 1963. He received the B.S. degree in electrical engineering and physics from Rice University, Houston, TX, in 1986, and the M.S. and Ph.D. degrees in electrical engineering from the California Institute of Technology, in 1987 and 1992, respectively.

In 1993, he joined the faculty of the University of Virginia, Charlottesville, where he is currently an Associate Professor of electrical engineering. During the 2001–2002 academic year, he was a Fulbright Scholar with the Department of Microelectronics, Chalmers University of Technology, Göteborg, Sweden. His current research interests include submillimeter electronics, high-frequency instrumentation and measurement systems, and quasi-optical techniques for millimeter-wave power combining, imaging, and beam forming.